Available online at www.sciencedirect.com
ScienceDirect
Ceramics International 36 (2010) 1225–1231
CERAMICS INTERNATIONAL
www.elsevier.com/locate/ceramint

Electrochemical characterizations of Fe-substituted $LiNiO_2$ synthesized in air by the combustion method

MyoungYoup Song [a,*], IkHyun Kwon [a], Sungbo Shim [b], Ji Hong Song [c]

[a] Division of Advanced Materials Engineering, Department of Hydrogen and Fuel Cells, Research Center of Advanced Materials Development, Engineering Research Institute, Chonbuk National University, 664-14 1ga Deogjindong Deogjingu, Jeonju, 561-756, Republic of Korea
[b] Rolls-Royce Corporation, 2001 South Tibbs Ave, Speed Code W-08, Indianapolis, IN 46241 USA
[c] College of Arts and Sciences, Cornell University, 147 Goldwin Smith Hall, Ithaca, NY 14853, USA

Received 3 December 2008; received in revised form 23 August 2009; accepted 17 December 2009
Available online 28 January 2010

Abstract

The phases that appear in the intermediate reaction steps for the formation of lithium nickel oxide were deduced from XRD and DTA analyses. XRD analysis and electrochemical measurements were performed for $LiNi_{1-y}Fe_yO_2$ ($0.000 \le y \le 0.300$) samples calcined in air after preheating in air at 400 °C for 30 min. Rietveld refinement of the $LiNi_{1-y}Fe_yO_2$ XRD patterns ($0.000 < y \le 0.100$) was carried out from a $[Li,Ni]_{3b}[Li,Ni,Fe]_{3a}[O_2]_{6c}$ starting structure model. The samples of $LiNi_{1-y}Fe_yO_2$ with $y = 0.025$ and 0.050 had higher first discharge capacities when compared with $LiNiO_2$ and exhibited better or similar cycling performance at a 0.1 C rate in the voltage range of 2.7–4.2 V. The $LiNi_{0.975}Fe_{0.025}O_2$ sample had the highest first discharge capacity of 176.5 mAh/g and a discharge capacity of 121.0 mAh/g at $n = 100$. With the exception of Co-substituted $LiNiO_2$, such a high first discharge capacity has not been previously reported.

Keywords: Lithium ion battery; $LiNi_{1-y}Fe_yO_2$; Combustion method in air; Cation disordering

1. Introduction

Transition metal oxides, such as $LiMn_2O_4$ [1–3], $LiCoO_2$ [4–6], and $LiNiO_2$ [7–16] have been investigated as potential cathode materials for lithium secondary batteries. $LiMn_2O_4$ is a relatively low-cost material and does not bring about environmental pollution because it does not contain toxic elements. However, the cycling performance of $LiMn_2O_4$ is not good. $LiCoO_2$ has a large conductivity, and a high operating voltage. $LiCoO_2$ can be easily prepared but contains Co, an expensive element. $LiNiO_2$ is a very promising cathode material since it has a large discharge capacity and possesses both economic and environmental advantages. However, its preparation is very difficult when compared with $LiCoO_2$ and $LiMn_2O_4$.

During the preparation of $LiNiO_2$, it is known that $Li_{1-z}Ni_{1+z}O_2$ forms rather than stoichiometric $LiNiO_2$ [14,17–19]. This phenomenon is called cation disordering. The Ni^{2+} ion, which has an ionic radius similar to that of Li^+, occupies the Li sites, thereby destroying the ideally layered structure and preventing the easy movement of lithium ions that is required for their intercalation and deintercalation during cycling. Such a scenario results in a small discharge capacity and poor cycling performance.

To improve the electrochemical properties of $LiNiO_2$, Co [20,21], Al [22,23], Ti [24,25], Ga [26], Mn [27], and Fe [28–32] ions were substituted for nickel ions by synthesization in oxygen. Reimers et al. [28] studied the solid solution series of $LiFe_yNi_{1-y}O_2$ ($0.1 \le y \le 0.5$). They reported that cation disordering primarily occurred between Fe and Li and that the amount of Li that can be reversibly cycled decreases as y increases. Kanno et al. [29] synthesized $LiFe_{1-y}Ni_yO_2$ by an ion-exchange reaction and reported that the cycling capacities of the 4 V region decreased with increasing iron content. Prado et al. [31] studied cation distribution in $Li_{1-z}(Ni_{1-y}Fe_y)_{1+z}O_2$ electrode materials and reported that, for the largest y and z values, iron ions are simultaneously present in the slab and in the inter-slab space. Chappel et al. [32] investigated the

* Corresponding author. Tel.: +82 63 270 2379; fax: +82 63 270 2386.
E-mail address: songmy@jbnu.ac.kr (M. Song).

0272-8842/$36.00
doi:10.1016/j.ceramint.2010.01.008

magnetic and structural properties of the hexagonal solid solution $LiNi_{1-y}Fe_yO_2$ ($y \leq 0.3$) and showed that 3d cations are always present in the Li layers. They also reported that Fe ions preferentially exist at the Ni site when $y \leq 0.1$.

It is known that $LiNiO_2$ synthesized in an O_2 atmosphere has, in general, better electrochemical properties than $LiNiO_2$ synthesized in air. This is because synthesis in O_2 leads to a lower degree of cation disordering. However, the synthesis of $LiNiO_2$ in air reduces production costs because the fabrication process does not require equipment for atmospheric control. Broussely et al. [33] synthesized $Li_{1-z}Ni_{1+z}O_2$ with $z = 0$ by heating $LiOH{\cdot}H_2O$ and NiO powders in the appropriate ratio to about 700 °C in air. A semi-industrial process was devised in order to produce quantities of 200 kg per batch. Moshtev et al. [34] synthesized $LiNiO_2$ by heat-treating appropriate amounts of $LiOH{\cdot}H_2O$ and NiO at 650–800 °C under an air flow. $LiOH{\cdot}H_2O$ was used as supplied, while NiO was prepared by the gradual heating of nickel(II) hydroxycarbonate·H_2O up to 420 °C. Arai et al. [18] synthesized $Li_{1-z}Ni_{1+z}O_2$ by using mixtures of starting materials with excess lithium. The mixtures were calcined at 700–800 °C for 5–60 h in air. The calcined powder was ground and washed with distilled water for 2 h so as to remove un-reacted lithium compounds. Among the metal-substituted samples synthesized in air, Co and/or Mn substituted $LiNi_{1-y}M_yO_2$ exhibited improved electrochemical properties. $LiNi_{1-y}Co_yO_2$ ($0.2 \leq y \leq 0.3$) showed capacities larger than 180 mAh/g. Yoshido et al. [35] prepared electroactive $LiMn_{0.2}Ni_{0.8}O_2$ in air that showed a discharge capacity higher than 150 mAh/g. They also reported that, when Co was doped into $LiMn_{0.2}Ni_{0.8}O_2$, then $LiCo_yMn_{0.2}Ni_{0.8-y}O_2$ compounds with discharge capacities higher than 155 mAh/g were successfully prepared in air [36].

$LiNiO_2$ synthesized by the solid-state reaction method does not have a large discharge capacity and does not exhibit good cycling performance. These features are probably due to its poor crystallinity and a smaller fraction of the $LiNiO_2$ phase being present as the result of impurities. On the other hand, homogeneous mixing of the starting materials can be accomplished by the combustion method when nitrates as starting materials and urea as a fuel are mixed in distilled water by a magnetic stirrer. Such a process may lead to improved by crystallinity and a homogeneous particle size when the sample is synthesized.

Combustion synthesis, applied in the field of propellants and explosives, is a chemical reaction between metal salts and a suitable organic fuel, accompanied by an exothermic and self-sustaining chemical reaction [37]. Its processing feature is that an amount of initial heat is required to start the chemical reaction, which then supplies the energy required for the materials to react without the input of external energy [38].

The range of the substituted fraction, y, in $LiNi_{1-y}M_yO_2$ for many studies was $0.0 \leq y \leq 0.9$. A review of the results of these studies showed that the charge and discharge capacities decreased rapidly when $y > 0.025$, except in the case of Co substitution. When Fe is substituted for Ni, the capacity reduction was severe when $y \geq 0.100$. For this work, we chose $0.010 \leq y \leq 0.300$ as the range of y. This value of y is smaller than the substituted fractions used in previously reported studies.

In this work, $LiNi_{1-y}Fe_yO_2$ ($y = 0.000$, 0.010, 0.025, 0.050, 0.100, and 0.300) was synthesized by the combustion method in an air atmosphere. Such a process can lead to both homogeneous mixing of the starting materials and reduced production costs. The electrochemical properties of the resulting compounds were then measured.

2. Experimental

In order to synthesize $LiNi_{1-y}Fe_yO_2$ ($y = 0.000$, 0.010, 0.025, 0.050, 0.100, and 0.300) in air by the combustion method, lithium nitrate ($LiNO_3$, Aldrich Chemical, purity 98%), nickel hexahydrate ($Ni(NO_3)_2{\cdot}6H_2O$, Aldrich Chemical, purity 98%), and iron nonahydrate ($Fe(NO_3)_3{\cdot}9H_2O$, Aldrich Chemical, purity 98%) were used as the starting materials. The starting materials, in the desired proportions, were dissolved in distilled water and mixed with urea (NH_2CONH_2, Aldrich Chemical, purity 98%) as a fuel by means of a magnetic stirrer. The molar ratio of urea to nitrate was 3.6. This mixture was preheated in air at 400 °C for 30 min. For the synthesis of $LiNi_{1-y}Fe_yO_2$, the preheated mixture was calcined in air at 600–800 °C for 3–48 h. The heating and cooling rates were approximately 100 °C h^{-1}.

Phase identification of the synthesized samples was performed via X-ray diffractometry (XRD) using a Rigaku III/A X-ray diffractometer with Cu K_α radiation. The scanning rate was 8° min^{-1}, and the scanning range of the diffraction angle (2θ) was $10° \leq 2\theta \leq 80°$. The resulting peaks were refined by the Rietveld method using a GSAS program [39]. The peak shape was described by a pseudo-Voigt function. For each diffraction pattern, the scale factor, zero point, unit-cell dimensions, and atomic parameters were refined. Differential thermal analysis (DTA) was performed for the $LiNiO_2$ precursor (an intermediate) combusted at 400 °C for 30 min.

To measure the electrochemical properties, electrochemical cells were constructed which consisted of the prepared sample as the positive electrode, Li metal as the negative electrode, and 1 M $LiPF_6$ in a 1:1 (volume ratio) mixture of ethylene carbonate (EC) and diethyl carbonate (DEC) as the electrolyte. A Whatman glass fiber was used as a separator. The cells were assembled in a dry box filled with argon. To fabricate the positive electrode, the active material, acetylene black, and polyvinylidene fluoride (PVDF) binder dissolved in N-methyl-2-pyrrolidone (NMP) were mixed at a weight ratio of 85:10:5 and applied to Al foil. The electrochemical tests were performed at room temperature with a battery charge–discharge cycle tester at a 0.1 C rate in the voltage range of 2.7–4.2 V.

3. Results and discussion

Shown in Fig. 1 are the X-ray powder diffraction patterns for $LiNiO_2$ calcined under an O_2 stream and in air at 700 °C for 6 h after preheating in air at 400 °C for 30 min. The sample calcined in air has a phase with an α-$NaFeO_2$ structure (space group; $R\bar{3}m$); no impurities are evident. However, the sample

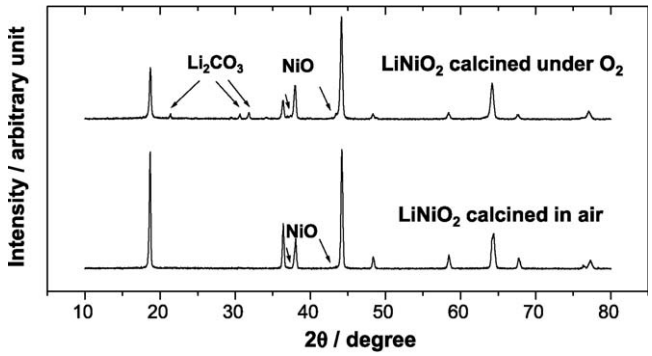

Fig. 1. X-ray powder diffraction patterns of $LiNiO_2$ calcined under an O_2 stream and in air at 700 °C for 6 h after preheating in air at 400 °C for 30 min.

calcined under an O_2 stream contains NiO and Li_2CO_3 in addition to the phase with an α-$NaFeO_2$ structure (space group; $R\bar{3}m$).

The X-ray powder diffraction patterns of $LiNiO_2$ calcined in air at 600–800 °C for 3–48 h after preheating in air at 400 °C for 30 min showed that the samples calcined at 600 and 650 °C had a phase with an α-$NaFeO_2$ structure (space group; $R\bar{3}m$). Except upon being calcined in air for 48 h, the samples also contained NiO and Li_2CO_3. As the calcination time was increased, the intensities of the peaks for the α-$NaFeO_2$ structure increased, while those for NiO and Li_2CO_3 decreased. The intensity of the (1 0 1) peak for the α-$NaFeO_2$ structure with good crystallinity was higher than that of the (0 1 2) peak. However, in the samples calcined at 750 and 800 °C, the intensity of the (1 0 1) peak was similar to or weaker than that of the (0 1 2) peak. Furthermore, the samples calcined at 800 °C showed less intense peaks than those calcined at 700 °C. The sample calcined at 700 °C for 3 h contained Li_2CO_3, but the samples calcined at 700 °C for 6 h or more did not contain any un-reacted materials and had similar XRD patterns, with the (1 0 1) peak being more intense than the (0 1 2) peak. Morales et al. [17] semi-quantitatively correlated the integrated intensity ratio of the (0 0 3) and (1 0 4) peaks with the lithium content in samples with $x < 0.9$. The ratio was later used by Ohzuku et al.

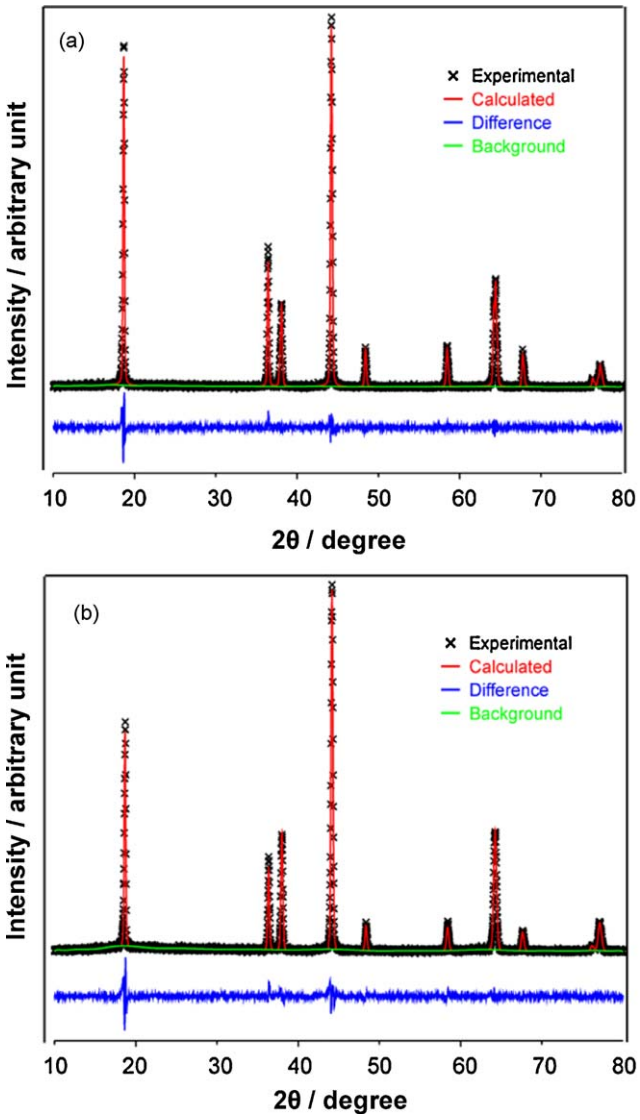

Fig. 2. Rietveld analysis results of $LiNiO_2$ calcined at (a) 700 °C for 12 h and (b) 800 °C for 12 h.

Table 1
Rietveld analysis results of $LiNiO_2$ calcined at 700 °C for various times.

Sample	R_p R_{pw} (%) R_b	a (Å)	b (Å)	c/a	Li_{3b}	Ni_{3b}	Li_{3a}	Ni_{3a}
700 °C, 3 h	7.7 90 3.0	2.890	14.221	4.920	0.8041	0.1559	0.0794	0.9206
700 °C, 12 h	7.2 9.1 2.1	2.885	14.214	4.927	0.8523	0.1477	0.0587	0.9413
700 °C, 24 h	7.7 10.2 2.2	2.889	14.226	4.924	0.3539	0.1403	0.0664	0.9336
750 °C, 6 h	9.1 7.5 2.2	2.893	14.229	4.919	0.7916	0.2084	0.0637	0.9363
800 °C, 12 h	7.5 9.6 3.3	2.895	14.235	4.917	0.7248	0.2752	0.0549	0.9451

[40] as a qualitative criterion for evaluating the stoichiometry of samples with $x > 0.96$. It is known that cation disordering decreases as the value of I_{003}/I_{104} increases. The values of I_{003}/I_{104} were 0.74, 0.98, 0.92, and 0.91 for the samples calcined for 3, 6, 12, and 24 h, respectively, showing that I_{003}/I_{104} value initially increased with increasing calcination time before tailing off. These results indicate that cation disordering decreased as the calcination time was increased from 3 to 6, 12, and 24 h.

Rietveld refinement was performed in order to evaluate the influence of calcining conditions on cation disordering. Since the radius of Li^+ (0.76 Å) and Ni^{2+} (0.69 Å) are similar, Ni and Li atoms are allowed to exchange 3a and 3b sites. Hence, a $[Li,Ni]_{3b}[Li,Ni]_{3a}[O_2]_{6c}$ model was used for the refinement. In Fig. 2, experimental and calculated peaks for the powder calcined at 700 °C for 12 h and at 800 °C for 12 h are shown along with their difference. The detailed refinement results are summarized in Table 1. Overall, the refinement yielded good agreement factors, which are represented by R_p, R_{pw}, and R_b. Low R_b values (2–3%) indicate that the structure model is robust. As the calcination temperature is increased above 700 °C, cation disordering, Ni migration from the 3a site to the 3b site, becomes more prominent. When the powder is calcined at 700 °C, cation disordering is reduced as the heat-treatment time is increased from 3 to 12 and 24 h. This result is in good agreement with the behavior of the I_{003}/I_{104} value with the hold time mentioned above. According to this result, control of the calcination temperature and the hold time is crucial for synthesizing good α-$NaFeO_2$-structured $LiNiO_2$.

Fig. 3 shows the DTA curve of the mixture for the synthesis of lithium nickel oxide combusted at 400 °C for 30 min. The peaks for the exothermic reaction are observed at about 500 and 675 °C. The peak for the endothermic reaction is observed around 735 °C.

For the synthesis of $LiNi_{1-y}Fe_yO_2$ $(0.000 \leq y \leq 0.300)$, mixtures of the starting materials with the desired compositions were calcined in an air atmosphere at 700 °C for 48 h after preheating them in air at 400 °C for 30 min.

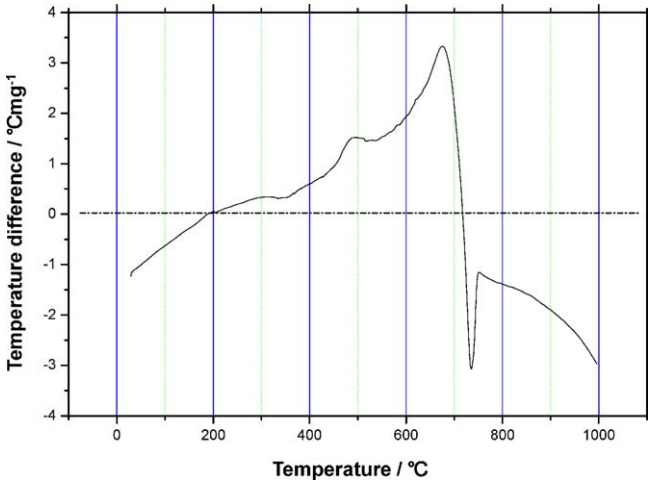

Fig. 3. DTA curve of a lithium nickel oxide precursor combusted at 400 °C for 30 min.

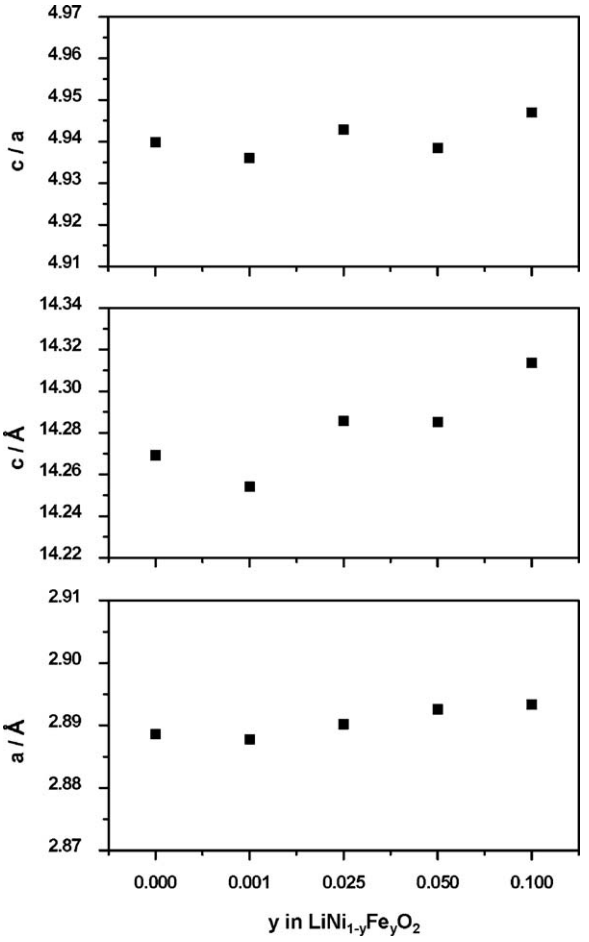

Fig. 4. Variations in the lattice parameters and their ratio with y in $LiNi_{1-y}Fe_yO_2$ $(0.000 \leq y \leq 0.100)$ calcined in air at 700 °C for 48 h.

The X-ray powder diffraction patterns of $LiNi_{1-y}Fe_yO_2$ $(0.000 \leq y \leq 0.300)$ calcined in air at 700 °C for 48 h after preheating in air at 400 °C for 30 min showed that all of the samples, with the exception of the sample with $y = 0.300$, had the phase with the α-$NaFeO_2$ structure of the rhombohedral system (space group; $R\bar{3}m$). Distinct splitting between the (0 0 6) and (0 1 2) peaks and between the (0 1 8) and (1 1 0) peaks was observed in the XRD patterns of these samples. This result suggests that the samples had a well-developed 2D layer structure and are electrochemically active [40].

Fig. 4 shows the variations in the hexagonal lattice parameters, the metal–metal intra-sheet distance (a), the metal–metal interlayer distance (c), and the trigonal distortion (c/a) with y in $Li_{1-z}(Ni_{1-y}Fe_y)_{1+z}O_2$ $(0.000 \leq y \leq 0.100)$ calcined in air at 700 °C for 48 h. A least squares refinement program, UnitCell [41], was used to retrieve the unit-cell constants from the diffraction data. The value of a for the sample with $y = 0.001$ is smaller than that for $LiNiO_2$ and increases as the value of y increases. The value of c for the sample with $y = 0.001$ is smaller than that for $LiNiO_2$ and increases gradually as the value of y increases. The value of c/a also tends to increase as the value of y increases.

Fig. 5 shows the variations in the discharge capacity at a 0.1 C rate with the number of cycles, n, for the $LiNi_{1-y}Fe_yO_2$

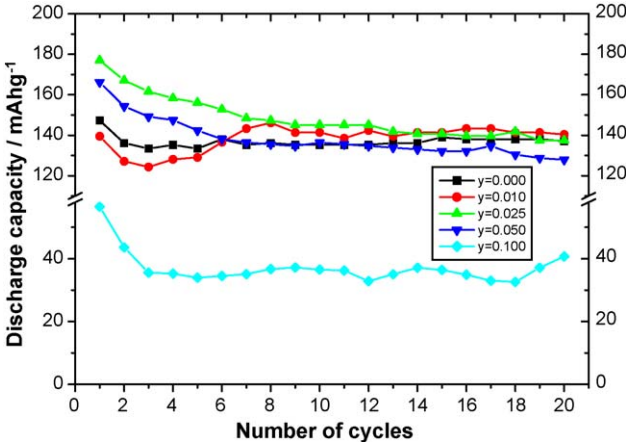

Fig. 5. Variations in the discharge capacity at a 0.1 C rate with the number of cycles in the voltage range of 2.7–4.2 V for $LiNi_{1-y}Fe_yO_2$ ($0.000 \leq y \leq 0.100$) calcined in air at 700 °C for 48 h.

($0.000 \leq y \leq 0.100$) calcined in air at 700 °C for 48 h in the voltage range of 2.7–4.2 V. The first discharge capacity decreases in the order of the samples with $y = 0.025$, 0.050, 0.000, 0.010 and 0.100. The discharge capacity of $LiNiO_2$ decreases at the second cycle, increases up to $n = 6$, then remains almost constant. The discharge capacity of the sample with $y = 0.010$ decreases up to $n = 3$, then increases up to $n = 7$ and does not vary thereafter. The increase in the discharge capacity with the increase in the number of cycles is considered to be due to the aging effect of the fabricated cathode. As time elapses, the contact of the cathode-constituting materials may improve, and the cathode may become stabilized as volatile materials, such as the binder, evaporate. The discharge capacities of the samples with $y = 0.025$ and 0.050 gradually decrease as the number of cycles increases. The sample with $y = 0.100$ has the smallest first discharge capacity of 56.6 mAh/g, and its discharge capacity decreases with increasing n. Through electrochemical impedance spectroscopy (EIS), Choi et al. [42] investigated the effects of cation disordering on electrochemical lithium intercalation involving the absorption and diffusion of lithium ion in porous $Li_{1-\delta}Ni_{1-y}Co_yO_2$ electrodes ($0 \leq \delta$; $y \leq 1$). They reported that the substituted Co ($0.2 \leq y \leq 0.3$) decreases the lattice size and makes the Ni^{2+} ions, which are larger than the Ni^{3+} ions, unstable. This prevents the Ni^{2+} ions from entering the Li sites and leads to the formation of $Li_{1-z}(Ni_{1-y}Co_y)_{1+z}O_2$ with z values that are nearly zero. Such a scenario results in improved electrochemical properties. Prado et al. [43] reported that the substitution of Fe for Ni in $LiNiO_2$ degrades the electrochemical properties by making the lattice size larger and, thus, making the Ni^{2+} ions more stable than Ni^{3+}. However, in this study, the samples with $y = 0.025$ and 0.050 have higher first discharge capacity than $LiNiO_2$ and exhibit better or similar cycling performance. In addition, the samples with $y = 0.025$ and 0.050 have higher discharge capacities than $LiNiO_2$ and exhibit cycling performances similar to that of $LiNiO_2$ from $n = 7$ through $n = 20$. The samples with $y = 0.000$, 0.010, 0.025, and 0.050 have much higher discharge capacities than the sample with $y = 0.100$ from $n = 1$ through $n = 20$. These samples show similar discharge capacities and good cycling performances from $n = 7$ through $n = 20$. $LiNi_{0.975}Fe_{0.025}O_2$ synthesized in air exhibits a higher first discharge capacity and higher discharge capacities than those synthesized in an O_2 atmosphere [44], and has the first discharge capacity similar to that of $LiNiO_2$ substituted by Co in air which had the highest first discharge capacity among the Co-substituted samples synthesized in air.

Fig. 6 shows the variations in the discharge capacity at a 0.1 C rate with the number of cycles, n, for $LiNi_{1-y}Fe_yO_2$ ($y = 0.000$ and 0.025) calcined in air at 700 °C for 48 h in the voltage range of 2.7–4.2 V. The variations were monitored from the first cycle to $n = 100$. The sample with $y = 0.025$ has a first discharge capacity of 176.5 mAh/g, and its discharge capacity decreases up to $n = 30$ (128.6 mAh/g), then remains almost constant. Its discharge capacity at $n = 100$ is 121.0 mAh/g. The sample with $y = 0.025$ has higher discharge capacities than $LiNiO_2$ up to $n = 20$, but, from $n = 20$ to $n = 100$, the discharge capacities are similar to those of $LiNiO_2$.

The variations, with the number of cycles, in the discharge capacities of $LiNiO_2$ synthesized by the combustion method (voltage range 2.7–4.4 V, 0.1 C rate) [45], the sol–gel method (voltage range 3.0–4.2 V, 0.05 C rate) [46], and the solid-state reaction method (voltage range 2.8–4.3 V, 0.1 C rate) [47] were compared. The $LiNiO_2$ synthesized by the combustion method had the highest first discharge capacity (189 mAh/g), followed, in order, by electrodes synthesized by the sol–gel method (169 mAh/g) and by the solid-state reaction method (145 mAh/g). From the fourth cycle, the $LiNiO_2$ synthesized by the sol–gel method had a higher discharge capacity than the sample fabricated by the combustion method. However, the two samples exhibited similar cycling performance, starting with the fourth cycle. The $LiNiO_2$ synthesized by the solid-state reaction method had a lower discharge capacity than that synthesized by the other methods. The solid-state sample also exhibited poor cycling performance. The small discharge capacity and the poor cycling performance of $LiNiO_2$ synthesized by the solid-state reaction method are believed

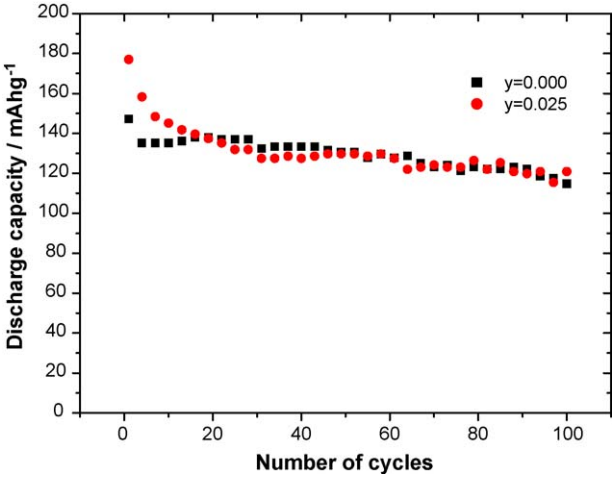

Fig. 6. Variations in the discharge capacity at a 0.1 C rate with the number of cycles in the voltage range of 2.7–4.2 V for $LiNi_{1-y}Fe_yO_2$ ($y = 0.000$ and 0.025) calcined in air at 700 °C for 48 h.

to be the result of poor crystallinity and poor particle size uniformity. Since the voltage ranges and the C-rates are different, a direct comparison is not possible. Nevertheless noteworthy, the $LiNiO_2$ electrode synthesized by the combustion method has the highest first discharge capacity, a relatively high discharge capacity, and relatively good cycling performance.

$LiCoO_2$ has a large conductivity and a high operating voltage. $LiCoO_2$ can also be easily prepared, as compared with $LiNiO_2$. Few results regarding $LiCoO_2$ synthesized by the combustion method and its electrochemical properties have been reported. Nitrates or carbonate were used as starting materials and urea, diformyl hydrazine ($C_2H_4N_2O_2$), or starch was used as fuel. The temperatures for preheating and calcination were 250–500 and 700–850 °C, respectively. The first discharge capacities were 42–123 mAh/g, and the particle size was 1–4 μm. Remarkable results were attained by Kalyani et al. [48]. They used starch as the combustion-assisting component. The synthesized particle size was less than 1.2 μm. The first discharge capacity of the synthesized $LiCoO_2$ was about 123 mAh/g at a current density of 0.1 mA/cm^2 in a voltage range of 3.0–4.2 V. A capacity fade of $<10\%$ up to the 30th cycle was observed.

$LiMn_2O_4$ is relatively inexpensive and does not bring about environmental pollution. For the synthesis of $LiMn_2O_4$ by the combustion method, nitrates and urea were used. The temperatures for preheating (or heating) and calcination were 200–600 and 400–800 °C, respectively. The first discharge capacities were 107–130 mAh/g. The $LiMn_2O_4$ synthesized by Yang et al. [49] had the highest first discharge capacity (130 mAh/g) and a discharge capacity at the 40th cycle of about 107 mAh/g at a constant current density of 0.3 mA/cm^2 in a voltage range 3.3–4.35 V (vs. Li). The spinel phase $LiMn_2O_4$ was synthesized by a combustion method under the following conditions: 0.60 molar ratio of urea to nitrate, 600 °C preset temperature of the furnace, and heat-treatment at 800 °C for 24 h. The synthesized powder had a uniform particle size distribution (80% of the particles were in the range of 4.5–9.0 μm). $LiMn_2O_4$ synthesized by the combustion method has a lower discharge capacity than $LiNiO_2$ synthesized by the combustion method.

In the DTA curve (Fig. 3) of the mixture for the synthesis of lithium nickel oxide combusted at 400 °C for 30 min, the peaks for the exothermic reaction were observed at about 500 and 675 °C. The peak for the endothermic reaction was observed around 735 °C. The XRD patterns showed that the sample calcined at 750 °C for 6 h contained a phase with the α-$NaFeO_2$ structure, NiO, and Li_2CO_3. The sample calcined at 650 °C for 6 h still contained a small amount of NiO and Li_2CO_3, but both of these phases disappeared after calcination for 48 h. The sample calcined at 700 °C for 6 h contained only the phase with the α-$NaFeO_2$ structure. In the samples calcined at and above 750 °C, the values of I_{003}/I_{104} decreased, indicating an increase in cation disordering. From these results, it is believed that the peak at about 500 °C corresponds to the formation of NiO and that the peak at about 675 °C corresponds to the temperature of the practical completion of the formation of lithium nickel oxide. The peak at about 735 °C is considered to be related to the melting of residual Li_2CO_3 present in the sample. Evaporation of Li_2O is expected at higher temperatures.

The combustion reaction at 400 °C and the reactions which occur as the temperature is increased may be written as follows:

$$\text{At } 400\,^\circ\text{C}: \ LiNO_3 + Ni(NO_3)_2\cdot 6H_2O + mCO(NH_2)_2 + (3m/2 - n/2)O_2 \rightarrow 1/2Li_2CO_3 + (1-n)NiO + nNi + (2m+6)H_2O + (m+3/2)N_2 + 15/4O_2 + (m-1/2)CO_2,$$

$$\text{At } 500\,^\circ\text{C}: \ 1/2Li_2CO_3 + (1-n)NiO + nNi + n/2O_2 \rightarrow 1/2Li_2CO_3 + NiO,$$

$$\text{At } 675\,^\circ\text{C}: \ 1/2Li_2CO_3 + NiO + 1/4O_2 \rightarrow LiNiO_2 + 1/2CO_2,$$

$$\text{At } 735\,^\circ\text{C}: \ \text{melting of residual } Li_2CO_3 \text{ present in the sample.}$$

where m is the number of moles of urea added, n is the number of moles of Ni produced, and x is the number of moles of Li evaporated.

4. Conclusions

The $LiNiO_2$ sample calcined in air has a phase with an α-$NaFeO_2$ structure (space group; $R\bar{3}m$) with no evidence of impurities, while the sample calcined under an O_2 stream contains NiO and Li_2CO_3 in addition to the phase with an α-$NaFeO_2$ structure. From the XRD and DTA analyses, the combustion reaction at 400 °C and the reactions which occur as the temperature was increased were proposed. Rietveld refinement of the XRD patterns of $LiNi_{1-y}Fe_yO_2$ ($0.000 < y \leq 0.100$) from a $[Li,Ni]_{3b}[Li,Ni,Fe]_{3a}[O_2]_{6c}$ starting structure model showed that cation disordering occurred in the samples. The samples of $LiNi_{1-y}Fe_yO_2$ with $y = 0.025$ and 0.050 had higher first discharge capacities than $LiNiO_2$ and better or similar cycling performance at a 0.1 C rate in the voltage range of 2.7–4.2 V. The $LiNi_{0.975}Fe_{0.025}O_2$ sample had the highest first discharge capacity of 176.5 mAh/g and a discharge capacity of 121.0 mAh/g at $n = 100$. Such a high first discharge capacity has not been previously reported, except for Co-substituted $LiNiO_2$. For some cathodes, an increase in the discharge capacity with cycling was observed over a specific range of cycle numbers. This is considered to be due to the aging effect of the fabricated cathode. As time elapses, the contact of the cathode-constituting materials may improve, and the cathode may become stabilized as volatile materials, such as the binder, evaporate.

Acknowledgement

This paper was supported by the selection of a research-oriented professor (Myoung Youp Song) at Chonbuk National University in 2009.

References

[1] J.M. Tarascon, E. Wang, F.K. Shokoohi, W.R. McKinnon, S. Colson, J. Electrochem. Soc. 138 (1991) 2859.
[2] A.R. Armstrong, P.G. Bruce, Lett. Nat. 381 (1996) 499.
[3] D.S. Ahn, M.Y. Song, J. Electrochem. Soc. 147 (3) (2000) 874.
[4] K. Ozawa, Solid State Ionics 69 (1994) 212.
[5] R. Alcátara, P. Lavela, J.L. Tirado, R. Stoyanova, E. Zhecheva, J. Solid State Chem. 134 (1997) 265.
[6] Z.S. Peng, C.R. Wan, C.Y. Jiang, J. Power Sources 72 (1998) 215.
[7] J.R. Dahn, U. von Sacken, C.A. Michal, Solid State Ionics 44 (1990) 87.
[8] J.R. Dahn, U. von Sacken, M.W. Juzkow, H. Al-Janaby, J. Electrochem. Soc. 138 (1991) 2207.
[9] A. Marini, V. Massarotti, V. Berbenni, D. Capsoni, R. Riccardi, E. Antolini, B. Passalacqua, Solid State Ionics 45 (1991) 143.
[10] W. Ebner, D. Fouchard, L. Xie, Solid State Ionics 69 (1994) 238.
[11] R. Kanno, H. Kubo, Y. Kawamoto, T. Kamiyama, F. Izumi, Y. Takeda, M. Takano, J. Solid State Chem. 110 (1994) 216.
[12] A. Hirano, R. Kanno, Y. Kawamoto, Y. Takeda, K. Yamaura, M. Takano, K. Ohyama, M. Ohashi, Y. Yamaguchi, Solid State Ionics 78 (1995) 123.
[13] A. Rougier, P. Gravereau, C. Delmas, J. Electrochem. Soc. 143 (1996) 1168.
[14] H. Arai, S. Okada, Y. Sakurai, J. Yamaki, Solid State Ionics 95 (1997) 275.
[15] M.Y. Song, R. Lee, J. Power Sources 111 (1) (2002) 97.
[16] M.Y. Song, I.K. Kwon, H.U. Kim, S.B. Shim, D.R. Mumm, J. Appl. Electrochem. 36 (2006) 801.
[17] J. Morales, C. Perez-Vicente, J.L. Tirado, Mater. Res. Bull. 25 (1990) 623.
[18] H. Arai, S. Okada, H. Ohtsuka, M. Ichimura, J. Yamaki, Solid State Ionics 80 (1995) 261.
[19] V. Ksenofontov, S. Reiman, D. Walcher, Y. Garcia, N. Doroshenko, P. Gutlich, Hyperfine Interact. 139/140 (2002) 107.
[20] A. Rougier, I. Saadoune, P. Gravereau, P. Willmann, C. Delmas, Solid State Ionics 90 (1996) 83.
[21] M.Y. Song, I.H. Kwon, H.U. Kim, J. Appl. Electrochem. 35 (2005) 1073.
[22] M. Guilmard, A. Rougier, M. Grune, L. Croguennec, C. Delmas, J. Power Sources 115 (2003) 305.
[23] M.Y. Song, R. Lee, I.H. Kwon, Solid state Ionics 156 (2003) 319.
[24] S.H. Chang, S.G. Kang, S.W. Song, J.B. Yoon, J.H. Choy, Solid State Ionics 86–88 (1996) 171.
[25] Y. Gao, M.V. Yakovleva, W.B. Ebner, Electrochem. Solid State Lett. 1 (1998) 117.
[26] Y. Nishida, K. Nakane, T. Stoh, J. Power Sources 68 (1997) 561.
[27] M. Guilmard, L. Croguennec, C. Delmas, J. Electrochem. Soc. 150 (10) (2003) A1287.
[28] J.N. Reimers, E. Rossen, C.D. Jones, J.R. Dahn, Solid State Ionics 61 (1993) 335.
[29] R. Kanno, T. Shirane, Y. Inaba, Y. Kawamoto, J. Power Sources 68 (1997) 145.
[30] M.Y. Song, D.S. Ahn, Solid State Ionics 112 (1998) 245.
[31] G. Prado, E. Suard, L. Fournes, C. Delmas, J. Mater. Chem. 10 (2000) 2553.
[32] E. Chappel, G. Chouteau, G. Prado, C. Delmas, Solid State Ionics 159 (2003) 273.
[33] M. Broussely, F. Perton, P. Biensan, J.M. Bodet, J. Labat, A. Lecerf, C. Delmas, A. Rougier, J.P. Peres, J. Power Sources 54 (1995) 109.
[34] R. Moshtev, P. Zlatilova, V. Manev, K. Tagawa, J. Power Sources 62 (1996) 59.
[35] M. Yoshido, Y. Torodov, K. Yamato, H. Noguchi, J.-I. Itoh, M. Okada, T. Mouri, J. Power Sources 74 (1998) 46.
[36] M. Yoshido, H. Noguchi, J.-I. Itoh, M. Okada, T. Mouri, J. Power Sources 90 (2000) 176.
[37] S.R. Jain, K.C. Adiga, V. Pai Verneker, Combust. Flame 40 (1981) 71.
[38] Y. Zhang, G.C. Stangle, J. Mater. Res. 9 (1994) 1997.
[39] A. Larson, R.B. von Dreele, Los Alamos Laboratory Report, 1994.
[40] T. Ohzuku, A. Ueda, M. Nagayama, J. Electrochem. Soc. 140 (1993) 1862.
[41] T.J.B. Holland, S.A.T. Redfern, Mineral. Mag. 61 (1997) 65.
[42] Y.M. Choi, S.I. Pyun, S.I. Moon, Solid State Ionics 89 (1996) 43.
[43] G. Prado, A. Rougier, L. Fournes, C. Delmas, J. Electrochem. Soc. 147 (8) (2000) 2880.
[44] I.H. Kwon, A study on the synthesis by the combustion method and the electrochemical properties of cathode materials $LiNi_{1-y}M_yO_2$ (M = Zn, Al, Ti and Fe) for lithium secondary battery, Ph.D. Thesis, Chonbuk National University, Republic of Korea, 2005.
[45] M.Y. Song, I.H. Kwon, H.U. Kim, S. Shim, D.R. Mumm, J. Appl. Electrochem. 36 (2006) 801.
[46] M.Y. Song, R. Lee, J. Power Sources 111 (2002) 97.
[47] D.S. Lee, A study on the synthesis and the electrochemical properties of $LiNi_{1-y}M_yO_2$ ($M = Zn^{2+}$, $A1^{3+}$ and Ti^{4+}) cathode materials for lithium secondary battery. Master Thesis, Chonbuk National University, Republic of Korea, 2004.
[48] P. Kalyani, N. Kalaiselvi, N. Muniyandi, J. Power Sources 111 (2002) 232.
[49] W. Yang, G. Zhang, J. Xie, L. Yang, Q. Liu, J. Power Sources 81–81 (1999) 412.